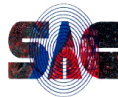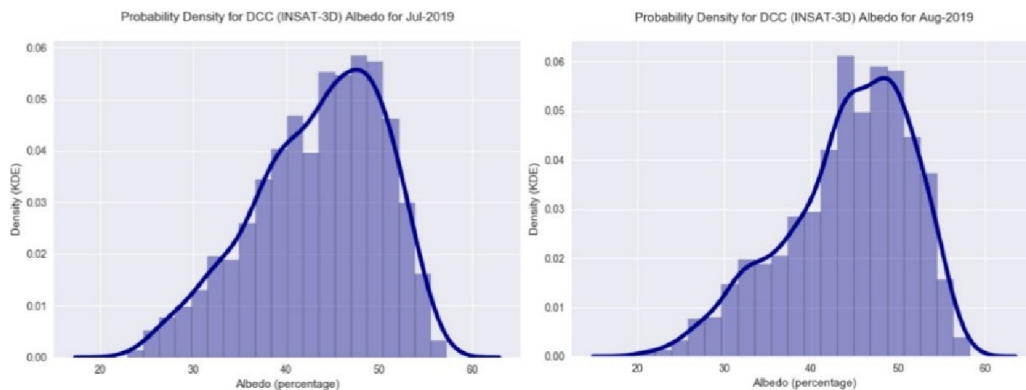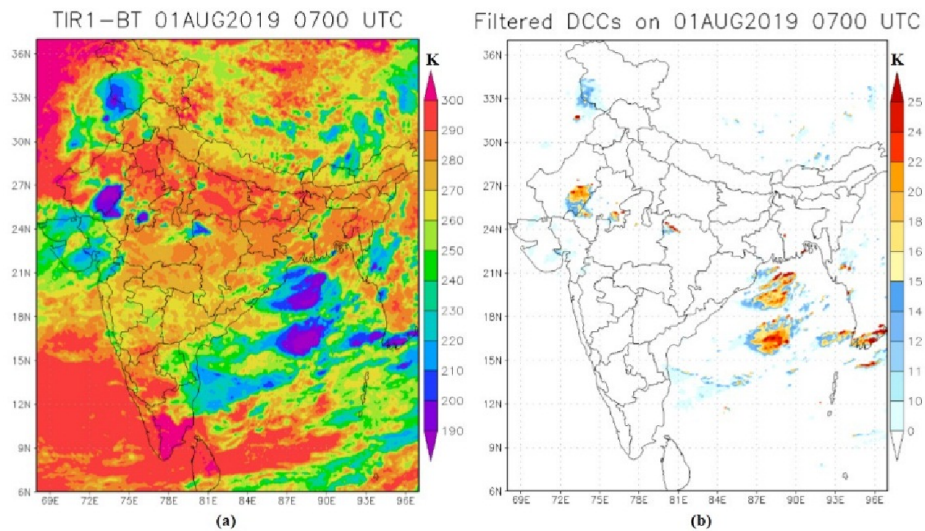# Calibration of INSAT-3D Visible Channel Data using Deep Convective Clouds: An Exploratory Study

Danish Hussain and K. N. Babu

CVD/EPSA, Space Applications Centre (SAC)

Indian Space Research Organization (ISRO)

Ahmedabad -380015

August-2020

Document Control and Data Sheet

1	Date	17 August, 2020
2	Title	Calibration of INSAT-3D Visible Channel Data using Deep Convective Clouds: An Exploratory Study
3	Version	1.0
4	Report Number	SAC/EPSA/CVD/SR/2020-05.
5	Type of Report	Scientific
6	No. of Pages	17
7	Authors	Danish Hussain and K. N. Babu
8	Origination Unit	CVD/EPSA, Space Applications Centre, Ahmedabad
9	Abstract	The possibility of using Deep Convective Clouds (DCCs) to calibrate INSAT-3D imager visible channel data is explored in this report. INSAT-3D imager data for 2019 is taken from the MOSDAC site and processed to get the radiances, albedo and water vapour (WV) & thermal infrared (TIR1) brightness temperature. Detection of DCCs is done using Brightness Temperature Difference (BTD) of WV and TIR1 channel data, the spatial homogeneity of DCCs, spatio-temporal-geographical criterion and solar geometrical-illumination conditions. Probability Density Function (PDF) of INSAT-3D DCC albedo peaks around 47.83%. The DCCs calibration gain coefficients are calculated using the mean value of RTM simulated DCC albedo reported in the literature [*Yeeun Lee el al, 2020 and Doelling el al 2013*]. Gain coefficients are in the range of *1.62 to 1.91*.
10	Classification	General
11	Circulation	Within EPSA

CONTENTS

Danish Hussain and K. N. Babu, "Calibration of INSAT-3D Visible Channel Data using Deep Convective Clouds: An Exploratory Study" (SAC/EPSA/CVD/SR/2020-05)

3

Abstract:

The possibility of using Deep Convective Clouds (DCCs) to calibrate INSAT-3D imager visible channel data is explored in this report. INSAT-3D imager data for 2019 is taken from the MOSDAC site and processed to get the radiances, albedo and water vapour (WV) & thermal infrared (TIR1) brightness temperature. Detection of DCCs is done using Brightness Temperature Difference (BTD) of WV and TIR1 channel data, the spatial homogeneity of DCCs, spatio-temporal-geographical criterion and solar geometrical-illumination conditions. Probability Density Function (PDF) of INSAT-3D DCC albedo peaks around 47.83%. The DCCs calibration gain coefficients are calculated using the mean value of RTM simulated DCC albedo reported in the literature [*Yeeun Lee el al, 2020 and Doelling el al 2013*]. Gain coefficients are in the range of *1.62 to 1.91*.

Introduction

INSAT-3D and INSAT-3DR are the geostationary satellites designed and developed by Indian Space Research Organization (ISRO) and were launched on 26th July 2013 and 8th September 2016 respectively. Both of the satellites have a 6 channel imager and a 19 channel sounder. The imager of each of the satellite operated from a geostationary altitude of 36000 km in visible (VIS) and shortwave infrared (SWIR) channels with 1 km spatial resolution, Mid-Wave infrared (MWIR) channel, Thermal-infrared-1 (TIR1) and Thermal-infrared-2 (TIR2) channels with 4 km spatial resolution and a water vapour (WV) channel with 8 km spatial resolution. The details of the imager channels are given in Table-1. Imager of both of the satellites provide data at 30 minute interval with a 15 minute difference of INSAT-3D and INSAT-3DR which means that imager data is available at every 15 minute time interval collectively.

Channel Number	Channel	Wavelength (µm)	Spatial Resolution (km)
1	VIS	0.55-0.75	1
2	SWIR	1.55-1.70	1
3	MWIR	3.8-4.0	4
4	WV	6.5-7.1	8
5	TIR-1	10.2-11.3	4
6	TIR-2	11.5-12.5	4

Table-1: Specifications of INSAT-3D and INSAT-3DR imager

INSAT-3D and INSAT-3DR are a series of multipurpose Geo-stationary satellites launched by ISRO to satisfy the telecommunications, broadcasting, meteorology, and search and rescue needs of India. The main objectives for these satellites are to provide an operational, environmental and storm warning system to protect life and property. INSAT-3D and INSAT-3DR are monitoring the earth's surface, oceanic surface observations and also provide data dissemination capabilities. It provides Broadcast Satellite Services (BSS) through two S-band transponders. The data acquisition and processing system is established at Space Applications Centre, Bopal Campus, Ahmedabad, India. The processing of INSAT-3DR data is taken place broadly in four steps. (1) Ground receiving system to receive data, (2) Data Reception (DR) system to generate raw data (L0) files, (3) Data Processing (DP) system to process L0 data and produce L1B data files (Calibrated and Geo located) and (4) Product generation and Dissemination system.

Regular monitoring of the performance of satellite sensors is a very important for the accurate and consistent estimation of geophysical parameters for different application purposes. For that purpose radiometric calibration is performed to determine consistently accurate radiometric observations over the period of lifetime of satellite sensor [M. Dinguirard & P.N. Slater 1999, and J.J. Butler & R.A. Barnes 1998]. To determine the consistent performance of the satellite sensors, pre-launch and post-launch calibration is performed [Chander G. el al 2010 & S. Belward 1999]. The pre-launch calibration is essentially a laboratory calibration exercise which is conducted in a controlled laboratory environment by using a well characterized radiation source. After the launch of satellite, post-launch calibration exercise is performed to determine the degradation in the performance of satellite sensor [W.A. Abdou 2002].

Different calibration exercises have been proposed for post-launch radiometric calibration of satellite sensors like lunar-calibration, on-board calibration, cross-calibration or inter-satellite calibration and vicarious calibration. On-board calibration is performed in-orbit satellites using sun, artificial black bodies and lamps. These black bodies are used as a source of calibration on-board satellite. But these extra black bodies and lamps increase the weight and cost of the satellite instrument and they cannot be controlled directly. Vicarious and cross-calibration techniques are widely used for the systems which do not have on-board calibrators. Also, these methods provide an independent validation tool for satellite sensors with on-board calibrators [6].

Calibration of visible satellite sensors is relied upon the characterisation of invariant targets like desert, moon, clear-sky Ocean, open ice sheets to determine the visible reflectance of the satellite sensors. However, this method cannot be applied to all of the operational satellite sensors. But, Deep Convective Clouds (DCCs) are viewed by all satellite sensors and are an invariant target for the calibration of satellite data, they can be characterized by the same satellite sensors which is under consideration.

DCCs are the optimal solar reflectors, are very common in the tropical regions, they are the brightest targets, they are located near the tropopause where the radiative impact of surface albedo effects, aerosols and water vapour absorption are minimum. They behave as an isotropic target under the non-oblique illumination and viewing conditions. They can be identified by using simple IR threshold techniques which make them ideal invariant target for the purpose of calibration. Thus, DCCs has the potential to calibrate the satellite imager data, in the visible channel, in a consistent and robust manner [Doelling el al 2013].

The present report presents a preliminary study to explore the possibility of using DCCs technique to calibrate INSAT-3D visible imager channel data. The study is conducted over the Indian region (0ºN-40ºN latitudes & 65ºE-98ºE longitudes) for the whole year of 2019. INSAT-3D albedo derived using channel-1 is used to calibrate visible channel and water vapour (WV) and thermal infrared-1 (TIR1), which are channel 4 and 5 respectively, are used to identify the deep convective clouds over the region of interest for 2019.

The structure of the report is as follow: (1) section data and methodology describes the details of the data used in the study and the techniques used for the detection of DCCs with a set of

criterion, (2) section results and discussions presents the detail findings of the study and a discussion about the same and (3) last section is conclusion and the scope for the future research.

Data and Methodology:

INSAT-3D level 1B (L1B STD) data is used in the present study. These data set has a temporal frequency of 0.5 hrs *i.e.* for every half an hour we have an INSAT-3D L1B STD file. Each file is approximately of size of 460 MB. For each 24 hours there are 48 files ideally. The data was taken from the MOSDAC website (www.mosdac.gov.in) and was processed to get the required albedo and brightness temperature values corresponding to visible, WV and TIR-1 channels respectively. For the other description about the INSAT-3D level-1 data and the conversion of counts to radiances and brightness temperature, interested readers can visit MOSDAC website to get INSAT-3D Algorithm Theoretical Basis Document which gives the details of the same (https://mosdac.gov.in/data/doc/INSAT_3D_ATBD_MAY_2015.pdf). The channels which are used are as follow: (1) Channel-1 (Visible) – this channel is used to get albedo values over the spatio-temporal domain of the study and (2) Channel-4 & channel-5 (WV & TIR1) brightness temperature these channels are used to detect deep convective clouds.

Deep Convective Clouds (DCCs) calibration technique is used in this work to calibrate visible channel of INSAT-3D imager. The first step for calibration is the identification of DCC pixels in the INSAT-3D imagery. The second step involves the processing of the identified DCC pixels for visible channel albedo for further statistical analysis to access the performance of the visible channel data. The procedure to identify DCC is based on a threshold of TIR1 and the brightness temperature difference (BTD) between WV and TIR1 channels of INSAT-3D. The pixels which are declared DCCs by using the criteria is known as Warm Water Vapor (WWV) pixels in the literature [Danish Hussain *el al* (2012) & Schmitz *et al* (1997)]. A brief description of physical basis of detection of DCCs using WWV pixel phenomena is as follow:

Under the influence of intense-active updrafts, deep convective systems can lift moisture and cloud particles to the top of the troposphere. The wind at the top can transport the moisture and cloud particles across the tropopause. Due to advection, cloud particles begin to move and fall due to their size and mass but moisture remain in the lower stratosphere. In lower stratosphere as the temperature increases with height, the emission from water vapour channel will include a contribution from moisture, which is at a temperature warmer than the top of the cloud. So there will be a positive difference between the brightness temperatures of the two channels i.e. (WV & TIR). Therefore, warmer the lower stratospheric moisture as compared to cold cloud top, higher will be the brightness temperature difference (BTD) between the two channels and this can be used as a signal to detect the deep convection from geostationary satellites which have water vapour (5.7 µm – 7.1 µm) and infrared window (10.5µm – 12.5µm) channels.

As mentioned earlier, the criteria to identify DCC is based on a threshold of TIR-1 and the brightness temperature difference (BTD) between WV and TIR1 channels of INSAT-3D along with the uniformity of the extracted area and the range of acceptable viewing zenith angle (VZA) and sun zenith angle (SZA). Only those pixels are declared as DCC for which following set of criteria is satisfied:

(1) DCCs are common over Inter-Tropical Convergence Zone (ITCZ). The geographical region considered is 30ºS to 30ºN for INSAT-3D disk.

(2) Only those pixels are taken which have TIR-1 Brightness Temperature (BT) TIR1-BT ≤ 220 K as well as the brightness temperature difference (BTD) between Water Vapor and TIR-1 channels satisfies: BTD = WV-BT − TIR1-BT ≥ 0.0

(3) To identify spatial homogeneity of the DCC only those pixels are declared as DCC for which the surrounding 3×3 pixels show a standard deviation of TIR1 BT less than 1K.

(4) To take into account the Bi-directional Reflectance Factor, only those pixels are taken for which VZA and SZA are in the range of 0º-30º.

After processing the above mentioned steps, we get DCC pixels. For these DCC pixels, albedo values were written in a file on monthly basis for further processing and statistical analysis. Probability Density Function (PDF) for each month of 2019 were generated using Kernel Density Estimation (KDE) method for all identified DCC pixel level albedo values with a bin size of 0.5% of the average DCC pixel albedo [David R. Doelling *el al* 2013]. It is a well-known fact, based on the Radiative Transfer Model (RTM) simulations, that for 0.65 μm satellite visible channel, PDFs of DCC pixel level albedo usually peaks around 78% to 85% [Doelling *el al* 2013, Sohn *el al* 2009 and Lee *et al* 2020]. This simulation observation is then compared to the PDFs of the INSAT-3D to obtain calibration of visible channel data.

Results and Discussions:

Figure-1(a) shows an example image of INSAT-3D TIR1 brightness temperature on 01 August 2019 over the Indian region. As August is a monsoon month for India, there are many convective activities over land and Bay of Bengal. The brightness temperature of TIR1 over many parts of Bay of Bengal vary between 190K and 210K approximately which is an indication of deep convective activity *i.e.* deep convective clouds. Some part of Rajasthan also have more or less the same values of TIR1 brightness temperature which shows the atmospheric deep convection.

Figure-1(b) shows the image of DCCs filtered using the criteria 1 to 4 mentioned in the previous section over the Indian region on 01 August 2019. The colour bar indicates the values of BTD. It is clear from the image that there are deep convective clouds over mid and north of Bay of Bengal and over some parts of south west of Rajasthan. There are some scattered DCCs are also there over north of Madhya Pradesh and mid Gujarat region. We have also generated images for the TIR1 brightness temperature and the filtered DCCs for Bay of Bengal which is shown in figure-2(a) and figure-2(b) respectively by which we can see and analyse the variation of BTD of these deep convective clouds.

Figure-3(a) and figure-3(b) shows the monthly Probability Distribution Functions (PDFs) constructed using INSAT-3D visible channel (0.55μm – 0.75μm) DCC pixel level albedo values for January-2019 to December-2019. The PDFs were generated using Kernel Density Estimation (KDE) method for all identified DCC pixel level albedo values with a bin size of 0.5% of the average DCC pixel albedo [David R. Doelling *el al* 2013]. Python matplotlib and

seaborn libraries are used to plot the PDFs. For kernel density estimation, the optimum value of bandwidth considered in the algorithm is 0.34 which is based on the range of the parameter under consideration.
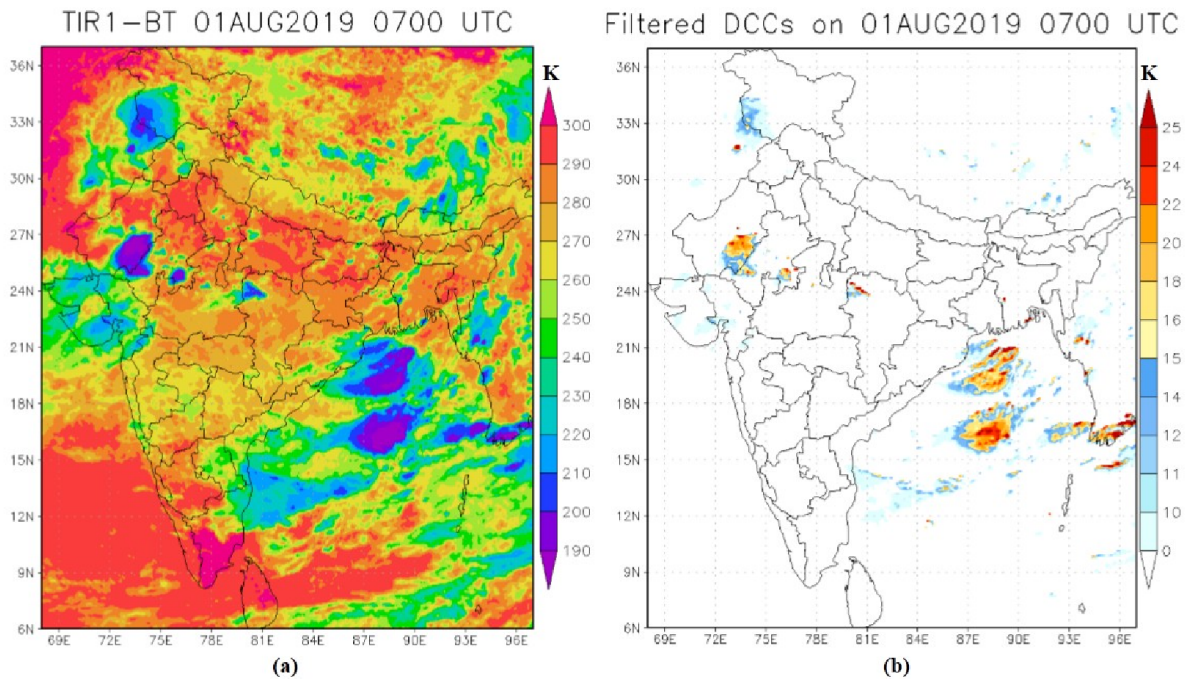

Figure-1: INSAT-3D (a) TIR1 Brightness Temperature and (b) Deep Convective Clouds filtered through the criteria used in the study. Colour bar in (b) represents the values of BTD between Water Vapour and TIR1 channels of INSAT-3D.

Figure-2: INSAT-3D (a) BoB TIR1 Brightness Temperature and (b) BoB Deep Convective Clouds filtered through the criteria used in the study. Colour bar in (b) represents the values of BTD between Water Vapour and TIR1 channels of INSAT-3D.
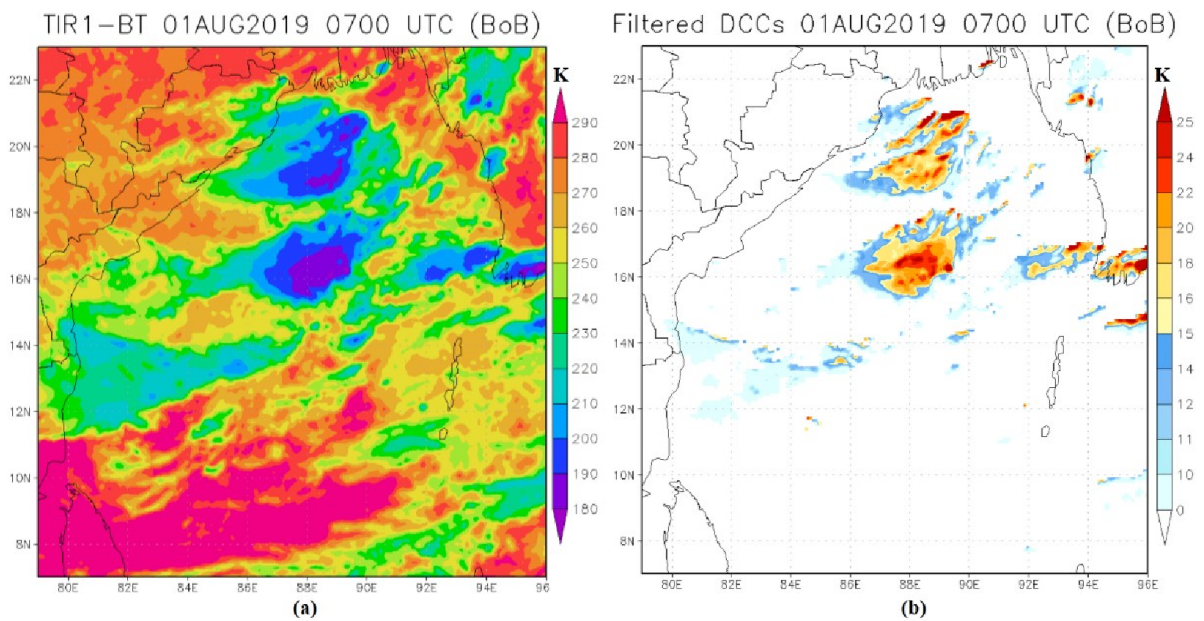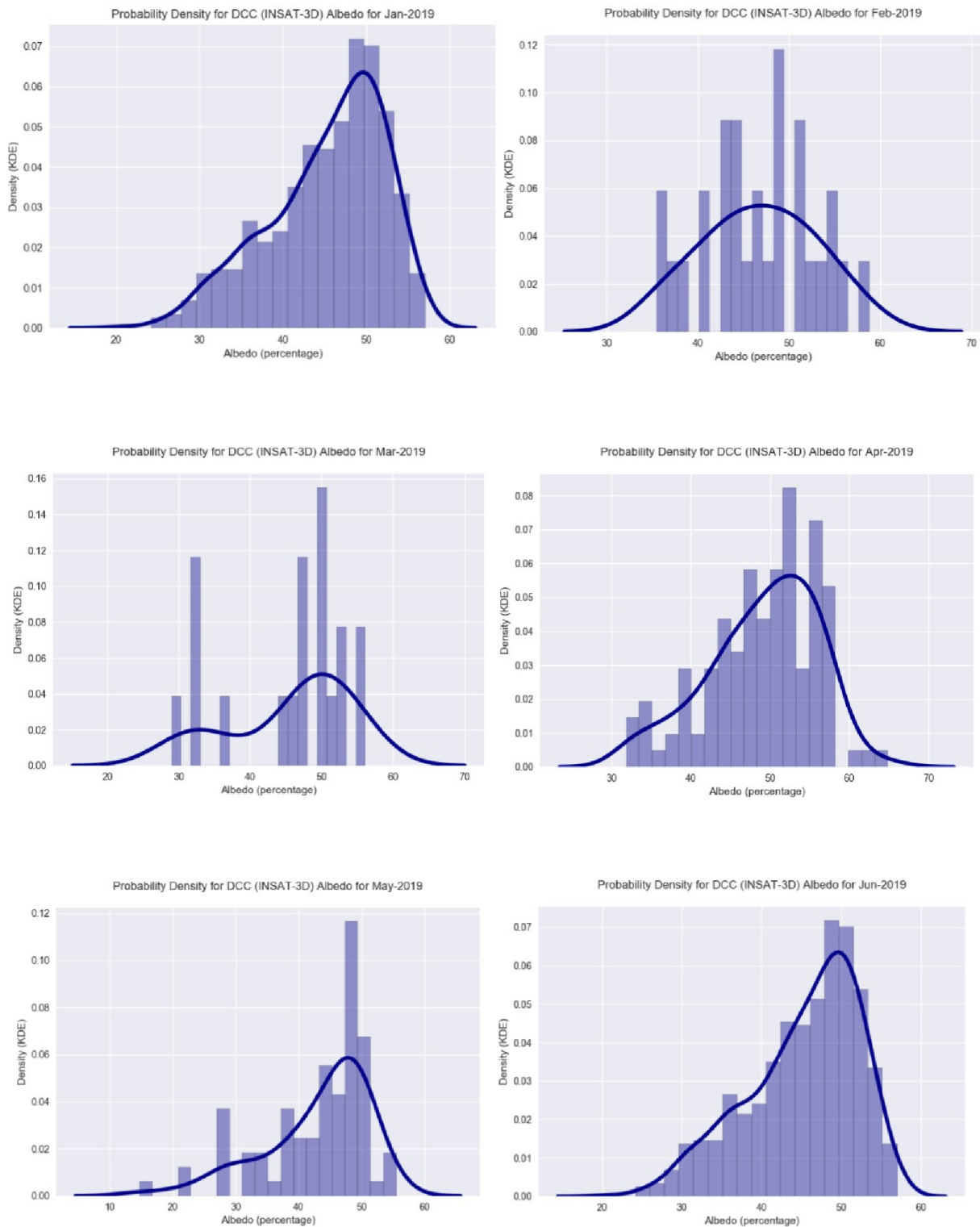
Danish Hussain and K. N. Babu, "Calibration of INSAT-3D Visible Channel Data using Deep Convective Clouds: An Exploratory Study" (SAC/EPSA/CVD/SR/2020-05)

9

Figure-3(a): Probability Density Functions of DCC pixel level albedo of INSAT-3D visible (0.55μm – 0.75μm) channel for January to June 2019. The probability density functions are calculated using Kernel Density Estimation (KDE) technique. For plotting, python matplotlib and seaborn libraries are used.

Figure-3(b): Probability Density Functions of DCC pixel level albedo of INSAT-3D visible (0.55μm − 0.75μm) channel for January to June 2019. The probability density functions are calculated using Kernel Density Estimation (KDE) technique. For plotting, python matplotlib and seaborn libraries are used.
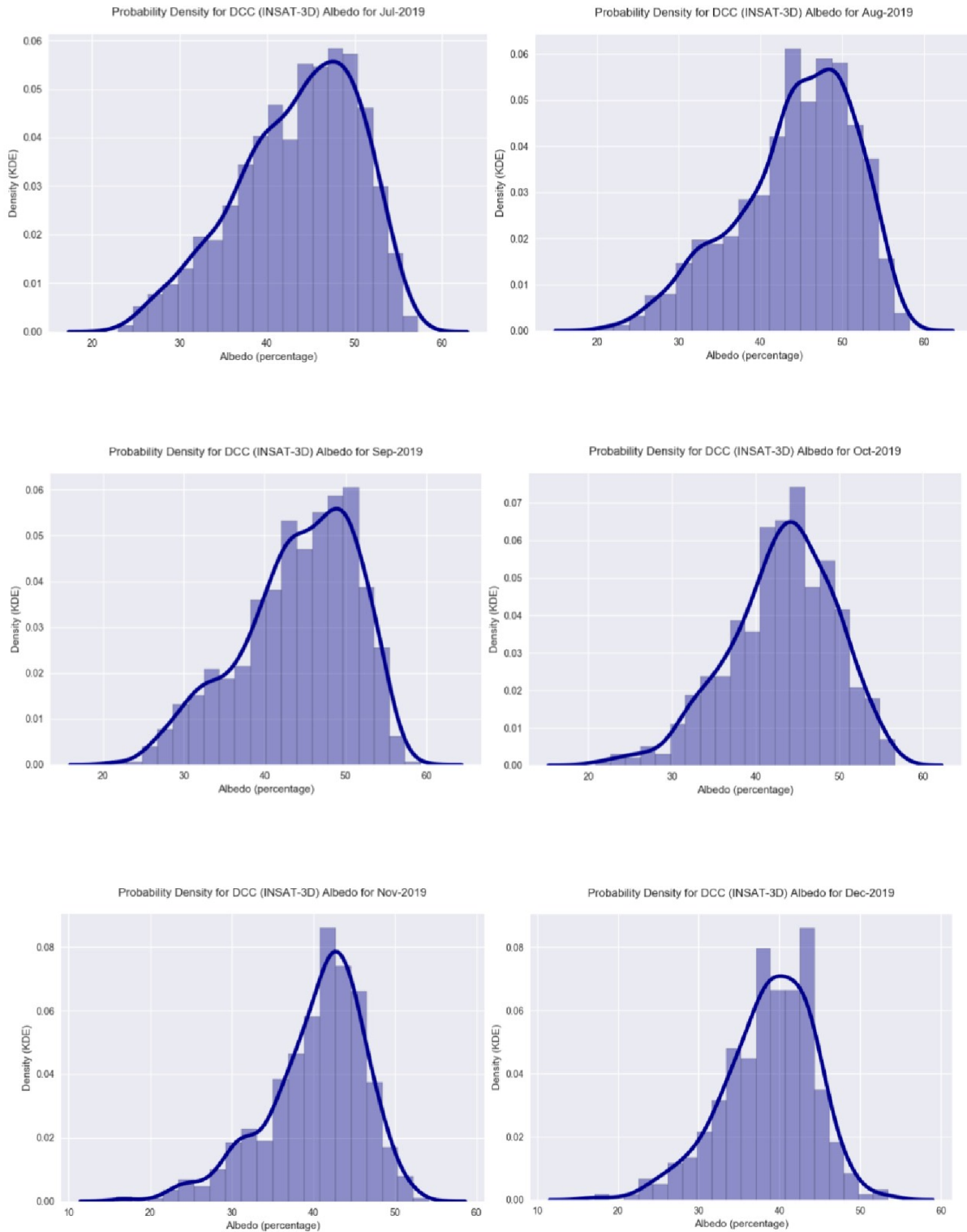
The peak of the PDFs for all of the months is more or less around 48%. The peak of January is at 50%, for February it is at 47%, for March at 50%, for April at 51%, for May at 48%, June at 50%, for July at 48%, for August 49%, for September at 49%, for October at 45%, for November at 44% and for December at 43%. *The mean peak for all of the months is at 47.83%.* RTM simulation of visible channel (0.65μm) imager data shows that the DCC albedo peaks around 82.5% on an average [Yeeun Lee *el al*, 2020 and Doelling *el al* 2013].

PDFs of DCC albedo are consistence from month to month which closely follows normal probability distribution. The PDFs also show that the DCC pixels of higher spatial homogeneity form the major proportion of the centre of the distribution. The data points in the tails are also there due to the unknown uncertain atmospheric effects. To analyse the tail of the distribution and it statistics, monthly DCC albedo *Kurtosis* is calculated.

Kurtosis is a statistical parameter of a probability distribution which shows the deviation of the tails of the distribution from the standard normal distribution. Positive higher values of kurtosis shows the heavy tails *i.e.* there are a plenty number of the data points are in the tails of the probability distribution and Negative higher values of kurtosis shows light tails of the probability distribution.

Figure-5 shows the monthly variation of Kurtosis of DCC albedo for 2019. Zero value on the x-axis means January-2019, 1 means February-2019 and so on. The variation of INSAT-3D visible channel DCC albedo is between -1 to 1 which shows light tails of the probability distribution functions which shows the DCC methodological technique is robust for the visible channel calibration purpose. *The Standard Deviation of the monthly kurtosis is 0.53%.*

Table-2 shows mean, mode and median of DCC pixel level albedo of INSAT-3D visible channel data from January to December 2019. The corresponding plots are shown in figure-4. Zero value on the x-axis means January-2019, 1 means February-2019 and so on. The variation of the three statistical parameters are in the range from 40% to 50%. *The Standard Deviation of Mean, Mode and Median are 2.2%, 2.16% and 2.23%* which are only two percent of the whole range and this shows the *temporal invariance of the DCCs* as the calibration targets.

Months of 2019	Mean	Mode	Median
Jan	43.80	45.62	45.65
Feb	46.71	44.46	46.89
Mar	45.66	47.33	48.00
Apr	49.08	45.13	50.40
May	43.02	48.55	45.71
Jun	45.26	49.33	46.79
Jul	43.45	45.52	44.35
Aug	44.22	48.15	45.22
Sep	44.18	48.06	45.02
Oct	43.13	46.10	43.76
Nov	40.32	41.51	41.60
Dec	41.66	43.86	43.07

Table-2: Mean, Mode and Median of INSAT-3D DCC pixel level albedo for whole of the months of year of 2019.
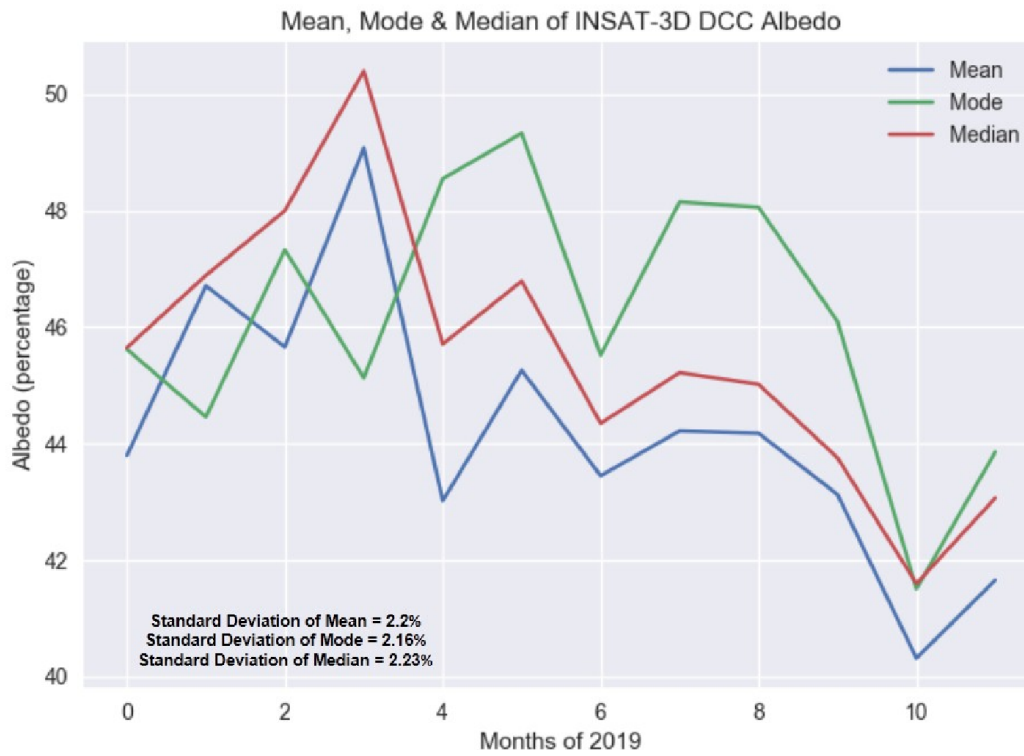
Figure-4: Monthly variation of mean, mode and median of DCC pixel level albedo of INSAT-3D visible channel data from January to December 2019.
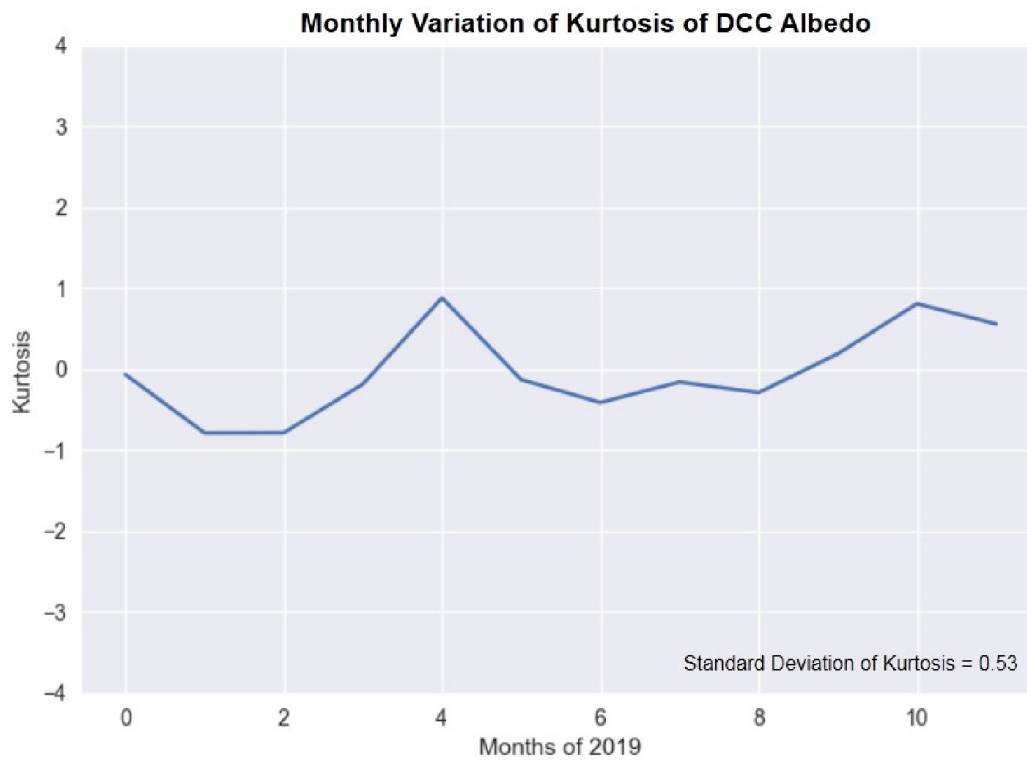

Figure-5: shows the monthly variation of Kurtosis of DCC albedo for 2019.
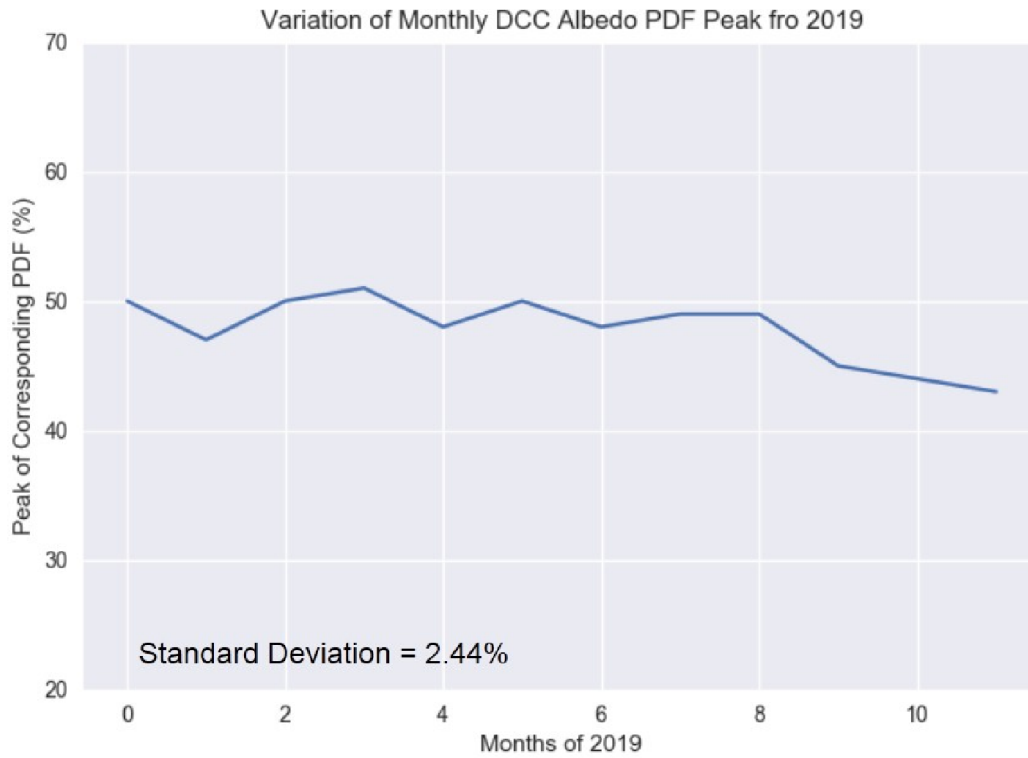
Figure-6: Variation of INSAT-3D DCC pixel level albedo probability density function peak values for 2019.
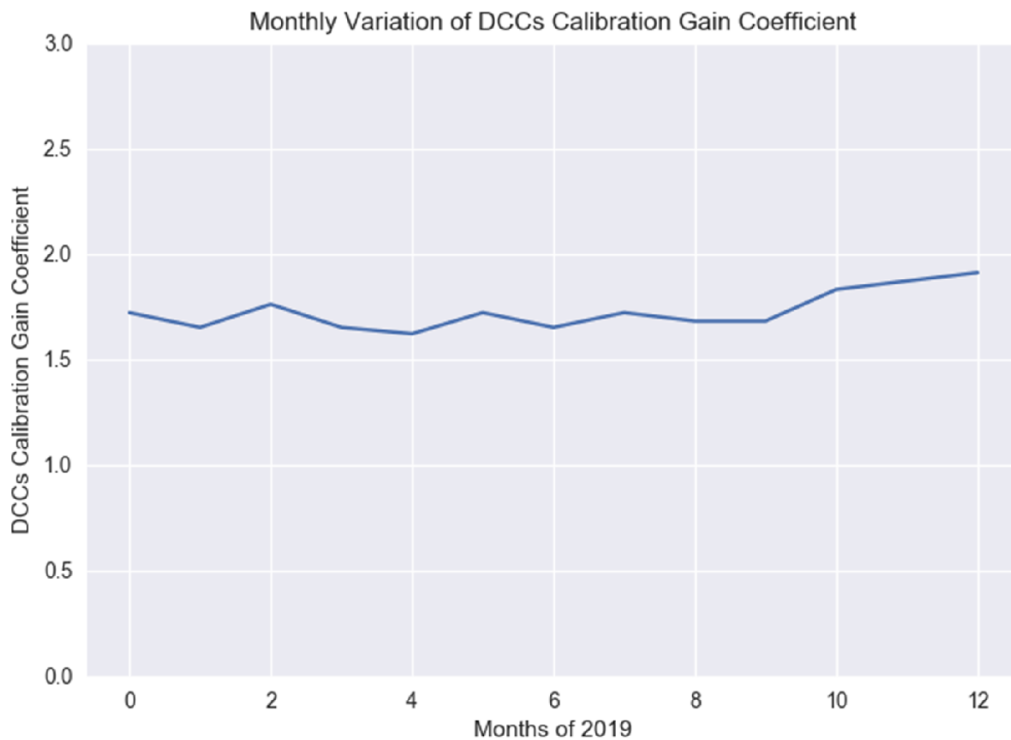

Figure-7: Monthly variation of DCCs calibration gain coefficient for 2019.

Variation of INSAT-3D DCC pixel level albedo probability density function peak values for 2019 is shown in figure-6. The *standard deviation of these PDF peak values is 2.44%* for 2019 which is consistent with the values of mean, mode and median values as shown in figure-5. The monthly variation of DCCs calibration gain coefficient is shown in figure-7. *The values of gain coefficients is in the range of 1.62 to 1.91*. The same is shown in table-3.

Months	INSAT-3D Albedo (%)	Standard RTM Avg. Albedo (%)	DCCs Cal. Gain Coefficient
Jan	50.02	82.5	1.65
Feb	47.14	82.5	1.75
Mar	50.10	82.5	1.65
Apr	51.17	82.5	1.62
May	48.03	82.5	1.72
Jun	50.14	82.5	1.66
Jul	48.11	82.5	1.71
Aug	49.15	82.5	1.69
Sep	49.03	82.5	1.68
Oct	45.17	82.5	1.82
Nov	44.18	82.5	1.87
Dec	43.20	82.5	1.91

Table-3: INSAT-3D Monthly DCCs calibration gain coefficients.

Conclusion and Future Scope:

The possibility of using Deep Convective Clouds (DCCs) to calibrate INSAT-3D imager visible channel data is explored in this report. INSAT-3D imager data for 2019 is taken from the MOSDAC site and processed to get the radiances, albedo and water vapour (WV) & thermal infrared (TIR1) brightness temperature. Detection of DCCs is done using Brightness Temperature Difference (BTD) of WV and TIR1 channel data, the spatial homogeneity of DCCs, spatio-temporal-geographical criterion and solar geometrical-illumination conditions. DCC albedo of INSAT-3D peaks around 47.83%.

The DCCs calibration gain coefficients are calculated using the mean value of RTM simulated DCC albedo reported in the literature [Yeeun Lee *el al*, 2020 and Doelling *el al* 2013]. RTM simulated albedo value is divided by the INSAT-3D peak PDF DCC pixel level albedo values which gives the DCCs calibration gain coefficients. Monthly DCCs calibration gain coefficients are obtained in this way and to see the variation, these gain coefficients are plotted in figure-7. Table-3 shows the values of the gain coefficients. It is clear from the table-3 and figure-7 that the DCCs calibration gain coefficients are in the range of 1.62 to 1.91.

As this work is an initial attempt to gain confidence in the DCC calibration technique to access the performance of INSAT imager visible channel data, there are more to be done to fully perform the desired calibration. The sensitivity of different DCCs detection method and different spatial homogeneity threshold with respect to mean, mode and median of DCC pixel level albedo, radiative transfer model simulation for DCCs albedo using a suitable Radiative

transfer Model and the comparison of the DCCs albedo between INSAT and other international satellite imager operated in the same band shall be the subject of our future work.

Acknowledgements

References:

[1] M. Dinguirard and P. N. Slater, "Calibration of space-multispectral imaging sensors: A review", *Rem. Sens. Environ.*, Vol.68, No.3, pp-194-205, Jun 1999.

[2] J. J. Butler and R. A. Barnes, "Calibration strategy for the Earth Observing System (EOS) – AM1 platform", *IEEE Trans. Geo. Rem. Sens.*, Vol. 36, No.4, p-1056, July 1998.

[3] David R. Doelling, Daniel Morstad, Benjamin R. Scarino, Rajendra Bhatt, and Arun Gopalan, "The Characterization of Deep Convective Clouds as an Invariant Calibration Target and as a Visible Calibration Technique", *IEEE Trans. Geo. Rem. Sens.*, Vol. 51, No.3, p-1147, March 2013.

[4] Chander G. et al, "Monitoring on-orbit calibration stability of the Terra MODIS and LANDSAT 7 ETMP sensors using pseudo-invariant test sites", *Rem. Sens. Environ.*, 114, 925-393.

[5] S. Belward, "International co-operation in the satellite sensor calibration: the role of the GEOS working group on calibration and validation", *Adv. Space Res.*, Vol.23, No.8, p-1443, January 1999.

[6] W.A. Abdou et al, "Vicarious calibration experiment in support of the multi-angle imaging spectroradiometer" *IEEE Trans. Geo. Rem. Sens.*, Vol. 40, No.7, p-1500, July 2002.

[7] Danish Hussain, C.M. Kishtawal and P.K. Pal, "Detection of Deep Convective Systems from Kalpana-1-VHRR: A Step towards forecasting of Thunderstorms from INSAT-3D Imager and Sounder", *SAC/EPSA/AOSG/ASD/SR/16/2012*, December 2012.

[8] Schmetz J., Tjemkes S., Gube M. and L. van de Berg, "Monitoring deep convection and convective overshooting with METEOSAT", *Adv. Space Res.* Vol.19, No.3, p-433, 1997.

[9] E. F. Vermote and Y. J. Kaufman, "Absolute calibration of AVHRR visible and near infrared channels using ocean and cloud views," *Int. J. Remote Sens.*, Vol.16, No.13, p-2317, 1995.

[10] P. Minnis, D. R. Doelling, L. Nguyen, W. Miller, and V. Chakrapani, "Assessment of the visible channel calibrations of the TRMM VIRS and MODIS on Aqua and Terra", *J. Atmos. Ocean. Technol.*, Vol.25, No.3, p-385, 2008.

[11] Babu, K. N., and Nandkishor, 2019. INSAT-3D and INSAT-3DR VIS and SWIR channel performance monitoring through top-of-the-atmosphere radiance over Desert and Ocean target. SAC/EPSA/CVD/SR/11, November 2019, 32pp.

[12] B. C. Kindel, P. Pilewskie, K. S. Schmidt, O. Coddington, and M. D. King, "Solar spectral absorption by marine stratus clouds: Measurements and modeling", *J. Geophys. Res.*, Vol.116, No.D10, p.D10203-1–D10203-16, 2011.